ON THE EARTHQUAKE MOTIONS FOR ASEISMIC DESIGNING

By

Kiyoshi KANAI,

Professor of Nihon University, Japan.

Abstract

The present investigation consists of two parts, the first part relates to the features of strong earthquake motions at bed rock computed from observed surface records and the second to the expectancy of the maximum velocity amplitude of earthquake motions at bed rock.

The results of the present investigation suggest that for the earthquake response analysis of big structures, based a considerable depth underground, the direct use of strong-motion seismograms observed at the surface is not always suitable.

Features of strong earthquake motions at bed rock

The strong-motion seismograms obtained to date in Japan and the U.S.A. have been used extensively for the response analysis of big structures. However, most of seismograms used for these analyses were obtained on or very near the ground surface. Thus, seismograms recorded at one site are not always adequate for the analysis of structures at other sites having different subsoil conditions or for big structures whose foundations are relatively deep.

To overcome these limitations, two methods have been developed to obtain the waveforms of strong earthquake motions under the ground. One method is by subsurface earthquake observation to get direct information of strong earthquake motions. However, there is little hope of obtaining a sufficient quantity of records of strong earthquakes under the ground in the near future because of the small number of observation stations. The second method is to estimate the waveforms of underground motions on the basis of those at the surface by application of the theory of multiple reflections of waves in the layered ground.[1)]

This chapter is concerned with the second method and presents results of computation for the waveforms of underground motion, in which most of the predominant surficial vibrations at the observation site have been eliminated, on the basis of strong-motion seismograms recorded in Japan and the U.S.A. The derived response spectra of the linear single mass system from both the original and computed waveforms are also presented for comparison of their effects on structures.

The relation between the waveforms of earthquake motions at the ground surface, $U_s(t)$, and those at a point in the first layer of the ground, $U_1(t)$, has been obtained as follows[2)];

$$U_1(t-\tau) = \frac{1}{2}\left[U_s(t) + U_s(t-2\tau)\right] \qquad (1)$$

where, τ is z/V_1 and, z and V_1 respectively are the depth in question from the surface and the propagation velocity of waves in the first layer. For the lower boundary of the layer, τ_1 is equal to H_1/V_1, in which H_1 is the thickness of the layer, and then the value of τ_1 may be estimated from the predominant period of earthquake motions or microtremors observed on the surface, T_s, by using the relation, $T_s = 4\tau_1$. Good applicability of this simple equation to actual seismograms has been proved by comparison of earthquakes observed underground and on the surface as shown in Fig. 1[3]. Fig. 1 not only exhibits how the weak layer near the surface plays an important role in the modification of seismic waves but also shows that the method is valuable in gaining information of the earthquake motions under the ground.

Numerical computations by the above-mentioned method were made for 10 strong earthquake records obtained at 5 stations in Japan and the U.S.A. Some of the data relating to these records are listed in Table 1. The original acceleration records in both analogue and digital forms were used in the investigation, and their sources are indicated in Table 1. For the digital records of El Centro (1940) and Taft (1952) consisting of only maxima and minima, given by G. V. Berg, cosine-curve interpolation method was applied. As for the analogue records, the digitization of amplitudes at about 1/100 sec intervals was performed.

Table 1. Strong earthquake records treated in the investigation.

No.	Station	Date	Orientation	Max. Accel. (gal)	$4\tau_1$	Remarks
1	Kushiro	Apr. 23, 1962	N159E N69E	385 240	0.30	B
2	Hoshina	Apr. 5, 1966	NS EW	220 420	0.10	C
3	Wakaho	Apr. 5, 1966	NS EW	260 250	0.40	C
4	El Centro	May 18, 1940	NS EW	330 230	0.23, 0.50	A
5	Taft	July 21, 1952	NS EW	180 150	0.29	A

A: K. Muto et al., "Digital Values for Analog Computation by SERAC," Preprint of SERAC Report No. 6, (1964). B: Strong-Motion Earthq. Obs. Comm., "Strong-Motion Earthquake Records in Japan," Vol. 2 (1965). C: Strong Earthq. Motion Obs. Center, ERI, "Strong Earthquake Motion Records in Matsushiro Earthquake Swarm Area," (1967).

Using data from Table 1, acceleration spectra of the linear single mass system of 10 different records are presented in Fig. 2 for 5% and 10% of critical damping. Among the spectra for the observed records, those of El Centro (1940), and Taft (1952), are from the SERAC report[4]. The values of $4\tau_1$ used for each observation site are indicated in the sixth column of Table 1. For the El Centro record, two different values of $4\tau_1$ were adopted because

two distinct periods appear on the record. Fig. 2 shows that the shapes of response curves for the computed waveforms exhibit a tendency to flatten as a whole, and the amplitudes of response at the neighborhood of the predominant period of the ground diminish to 1/2-1/5 compared with those of the original record at the surface.

As might be expected, results of the computation show that there is much and significant difference between the waveforms of earthquake motions under the ground and on the surface with respect to the dynamic response of structures. This would suggest that for the earthquake response analysis of big structures, based a considerable depth underground, the direct use of strong-motion seismograms observed at the surface is not always suitable.

Maximum velocity amplitude of earthquake motions at bed rock

Some of the results of the recent investigations told us that the damage to structures caused by earthquake motions depends mostly on the velocity amplitude of earthquake motions. However, big structures are founded generally on a competent subsurface formation capable of supporting them, so the intensity of earthquake motions at bed rock is still important in the direction of earthquake engineering. Therefore, in this paper, the expectancy of the velocity amplitude of earthquake motions at bed rock in Japan is investigated statistically by using an empirical formula for the velocity amplitude of earthquake motions at bed rock and the table concerning the magnitude as well as the origin of major earthquakes in and near Japan which were accompanied by damage.

The empirical formula used here is as follows;

$$\log_{10} v_0 = 0.61M - \left(1.66 + \frac{3.60}{x}\right)\log_{10} x - \left(0.631 + \frac{1.83}{x}\right) \qquad (2)$$

in which v_0 , M and x represent the velocity amplitude of earthquake motions at bed rock in cm/sec, the magnitude of earthquake and hypocentral distance in km, respectively. Besides, Eq. (2) can be available for the range of periods 0.05 sec — 0.2 sec to T_m , and T_m is a function of magnitude as follows;

$$\log_{10} T_m = 0.39M - 1.70 \qquad (3)$$

In the practical calculation, the hypocentral depth being assumed at the most frequent value in the table, that is, 30 km, and the maximum velocity amplitude at the mesh points of 0.4 degree intervals of longitude and latitude being determined in 507 earthquakes. The expectancy of the maximum velocity amplitude of earthquake motions at bed rock may be obtained by the following formula

$$\frac{y}{Y}\sum_{\overline{v}}^{\infty} N(v) = 1 \qquad (4)$$

in which $\overline{v}$ and $N(v)$ are the expected value of the maximum velocity amplitude during y year and the frequency spectrum of velocity amplitude v , respectively,

and Y is the length of the historical time of earthquakes. In the present paper, T are 1290, 1140 and 220 years for south west, north east and Hokkaido districts, respectively.

The final results for the expectancy of the maximum velocity amplitude of earthquake motions at bed rock in 75, 100 and 200 years are shown in Fig. 3. The maximum velocity amplitude of earthquake motions on the surface of ground may be obtained by multiplying the values represented in Fig. 3 by $5\sqrt[4]{T_G}$, in which, T_G represents the predominant period of ground in sec.

Acknowledgments

In conclusion I wish to express my sincerest thank to Miss S. Yoshizawa, Dr. T. Tanaka and Mr. T. Suzuki with whose kind aid the present investigation was brought to a successful close. And also I wish to express sincere thanks to Prof. H. Umemura for use of the analogue computer SERAC.

The cooperation of Mr. T. Nishikawa, a graduate student of the University of Tokyo, in the computation of the response spectra is also gratefully acknowledged.

The computation in this study was carried out through the courtesy of the Computer Center of the University of Tokyo.

References

1) K. Kanai and S. Yoshizawa, Bull. Earthq. Res. Inst., 41(1963), 825-833.
E. Shima, Bull. Earthq. Res. Inst., 40(1962), 187-259
H. Kawasumi and E. Shima, Proc. Japan National Symp. Earthq. Engg. (1962), 13 (in Japanese).
H. Kobayashi and H. Kagami, Trans. Arch. Inst. Japan, Extra (1967), 163 (in Japanese).

2) K. Kanai and S. Yoshizawa, loc. cit., 1).

3) K. Kanai et al., Bull. Earthq. Res. Inst., 44(1966), 609-643.

4) Strong Earthq. Response Analysis Committee, SERAC Report No. 4 (1964), No. 6 (1966).

5) F. Neumann, Proc. II World Conf. Earthq. Engg., 1960,
I. Muramatsu, Sci. Rep. Gifu Univ., 3(1966), 470-481,
K. Kanai, Bull. Earthq. Res. Inst., 45(1967), 339-343.

6) K. Kanai et al., Bull. Earthq. Res. Inst., 44(1966), 1276.

7) T. Usami, ditto, 44(1966), 1571-1622. (in Japanese)

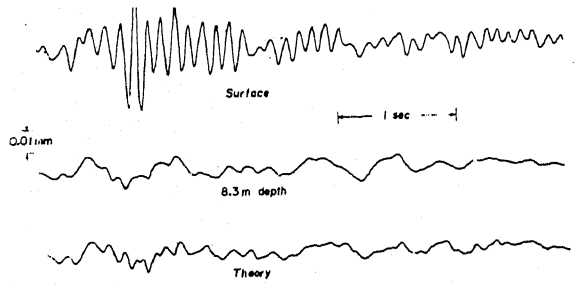

Fig. 1a. Tsuruga, Fukui

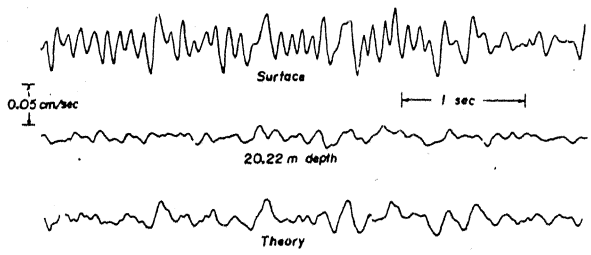

Fig. 1b. Futaba, Fukushima

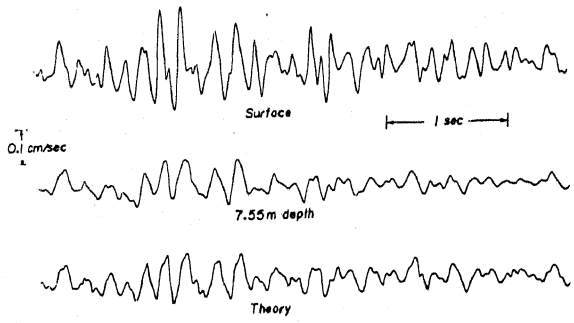

Fig. 1c. Oarai, Ibaraki

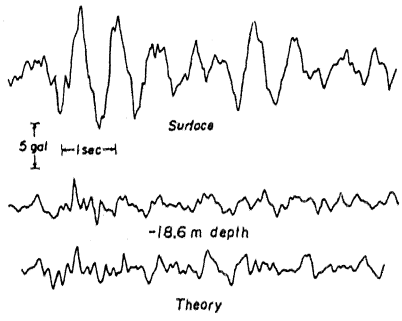

Fig. 1d. Marunouchi, Tokyo

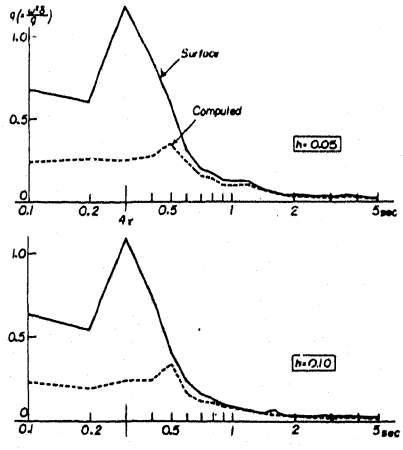

Fig. 2a. Kushiro, N159E

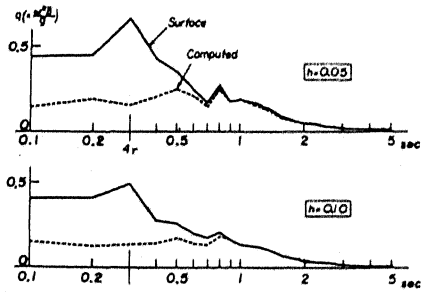

Fig. 2b. Kushiro, N69E

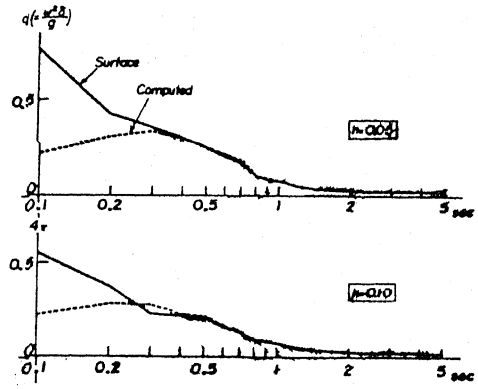

Fig. 2c. Hoshina, NS

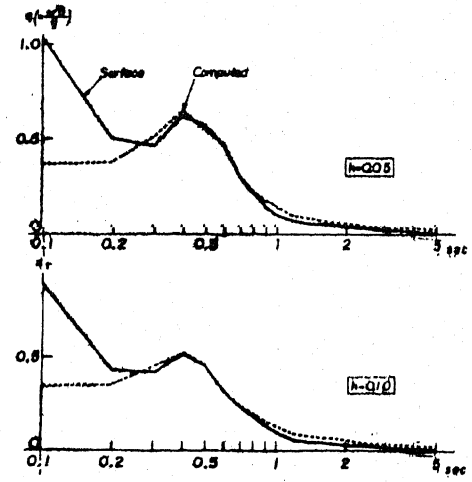

Fig. 2d. Hoshina, EW

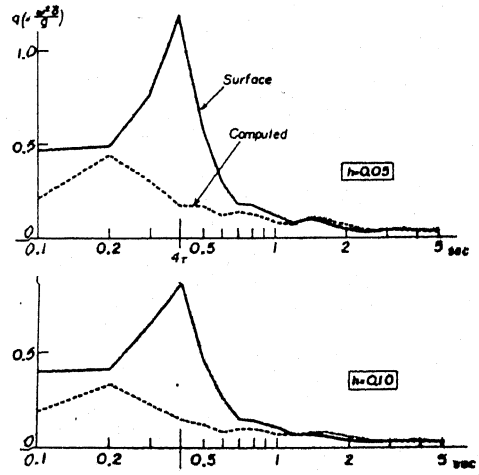

Fig. 2e. Wakaho, NS

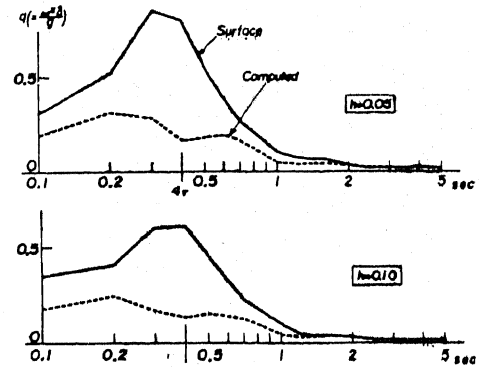

Fig. 2f. Wakaho, EW

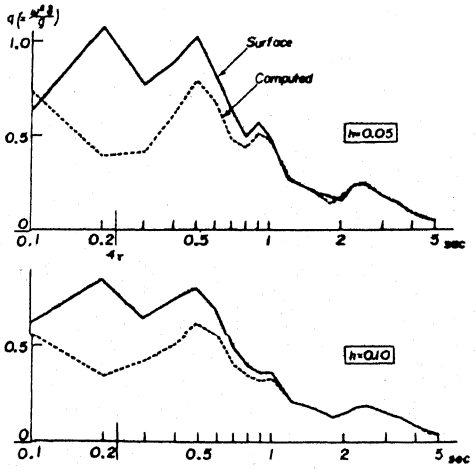

Fig. 2g. El Centro, NS (0.23 sec)

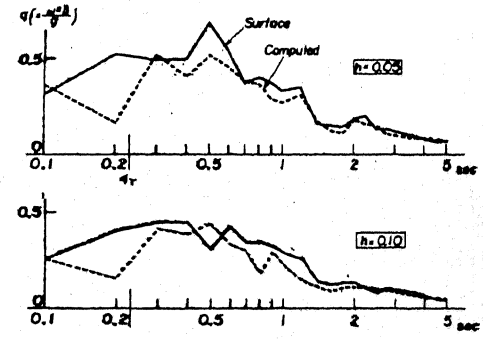

Fig. 2h. El Centro, EW (0.23 sec)

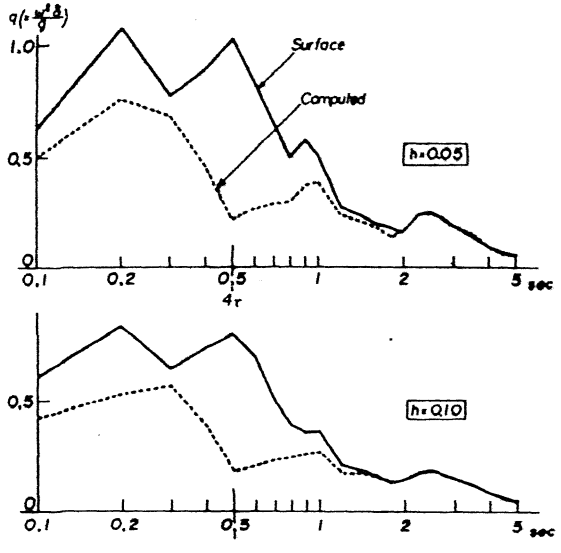

Fig. 2i. El Centro, NS (0.50 sec)

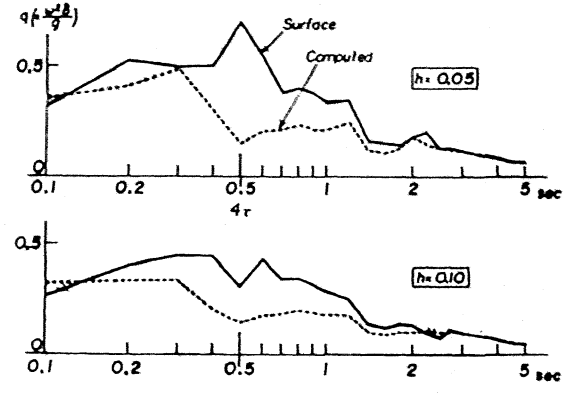

Fig. 2j. El Centro, EW (0.50 sec)

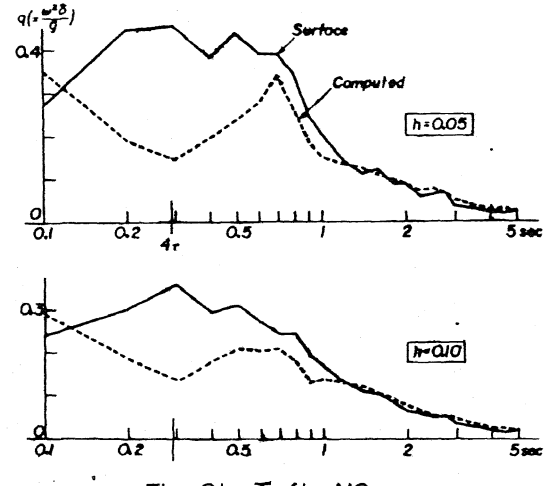

Fig. 2k. Taft, NS

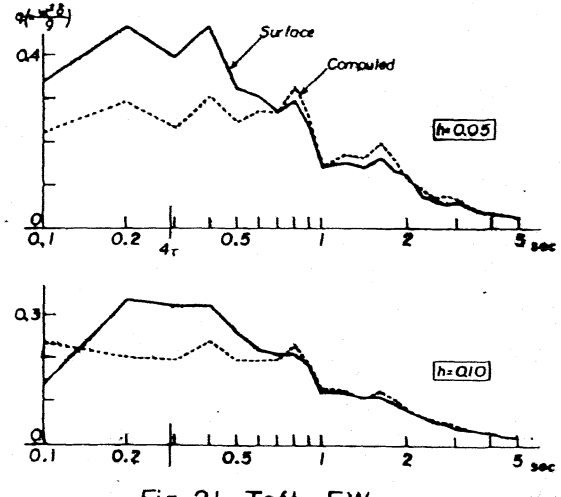

Fig. 2l. Taft, EW

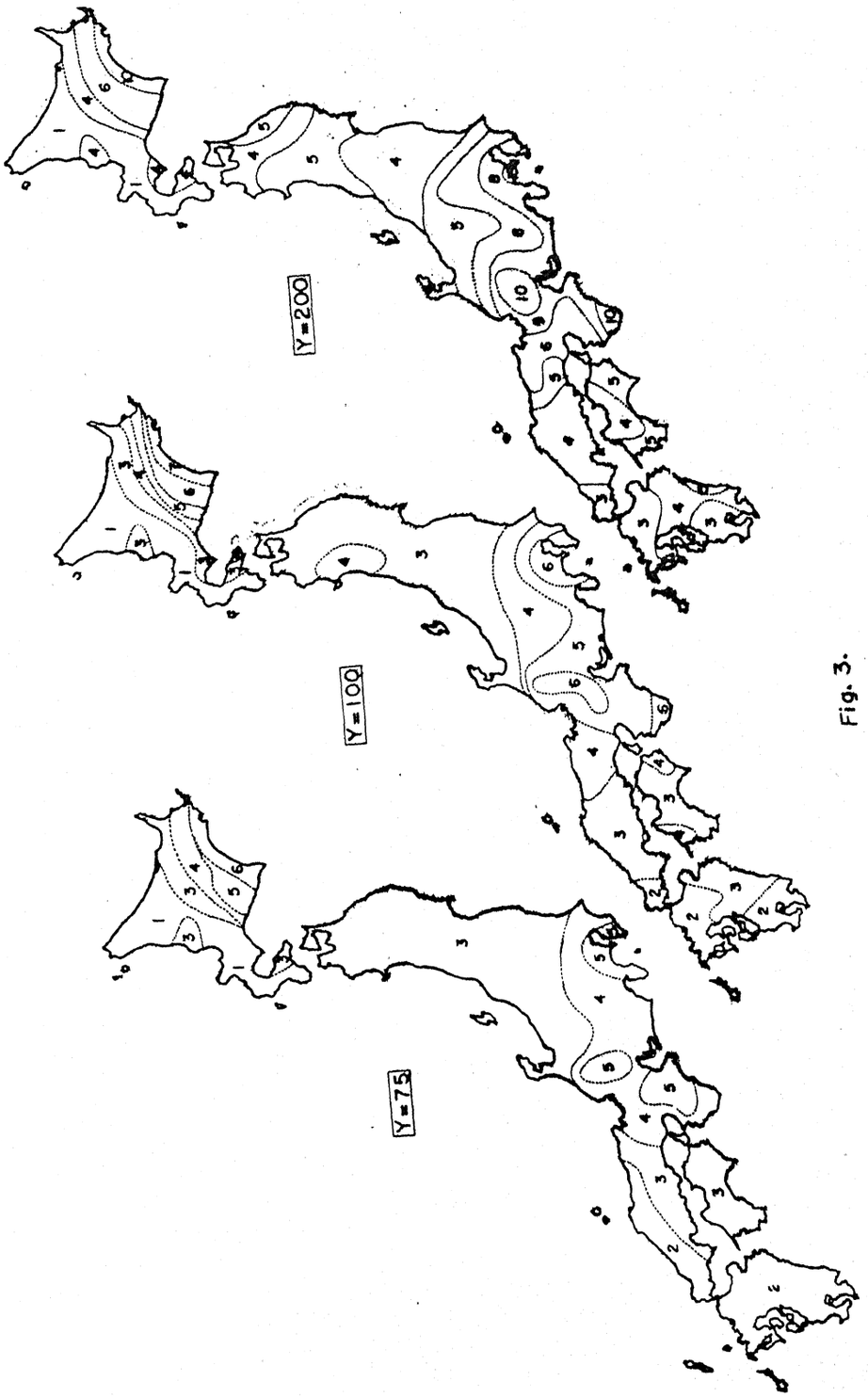

Fig. 3.